

UC Riverside

UC Riverside Previously Published Works

Title

Kaempferol Treatment after Traumatic Brain Injury during Early Development Mitigates Brain Parenchymal Microstructure and Neural Functional Connectivity Deterioration at Adolescence.

Permalink

<https://escholarship.org/uc/item/70x1g5gx>

Journal

Journal of neurotrauma, 37(7)

ISSN

0897-7151

Authors

Parent, Maxime
Chitturi, Jyothsna
Santhakumar, Vijayalakshmi
[et al.](#)

Publication Date

2020-04-01

DOI

10.1089/neu.2019.6486

Peer reviewed

Kaempferol treatment after TBI during early development mitigates brain parenchymal microstructure and neural functional connectivity deterioration at adolescence

Maxime Parent¹, Jyothsna Chitturi⁵, Vijayalakshmi Santhakumar^{2,3}, Fahmeed Hyder^{1,4},
Basavaraju G. Sanganahalli¹, Sridhar S. Kannurpatti^{5*}

¹Department of Radiology and Biomedical Imaging, Yale University School of Medicine, 330 Cedar St, New Haven, CT 06520

²Department of Pharmacology, Physiology and Neuroscience, Rutgers Biomedical and Health Sciences-New Jersey Medical School, Medical Science Building, 185 South Orange Ave, Newark, NJ 07101

³Department of Molecular, Cell and Systems Neuroscience, University of California at Riverside, Riverside, CA 92521

⁴Department of Biomedical Engineering, Yale University, 10 Hillhouse Ave, New Haven, CT 06520

⁵Department of Radiology, Rutgers Biomedical and Health Sciences -New Jersey Medical School, ADMC-5 Room 575, 30 Bergen St, Newark, NJ 07103

Maxime Parent, PhD, Postdoctoral Fellow¹

Tel: (203) 550-9852, Fax: (203) 785-6643; email: maxime.parent@yale.edu

Jyothsna Chitturi, PhD, Postdoctoral Fellow⁵

Tel: (973) 972-7417; Fax: (973) 972-7363; jyothsna.chitturi@rutgers.edu

Vijayalakshmi Santhakumar, MBBS, PhD, Associate Professor^{2,3}

Tel: (973) 972-2421; Fax: (973)-972-5059; email: santhavi@njms.rutgers.edu

Fahmeed Hyder, PhD, Professor^{1,4}

Tel: (203) 785-6205; Fax: (203) 785-6643; e-mail: fahmeed.hyder@yale.edu

Basavaraju G. Sanganahalli, PhD, Associate Research Scientist¹

Tel: (203) 785-6170; Fax: (203) 785-6643; e-mail: basavaraju.ganganna@yale.edu

Sridhar S. Kannurpatti, PhD, Assistant Professor⁵

Tel: (973) 972-7417; Fax: (973) 972-7363; email: kannursr@njms.rutgers.edu

Keywords: traumatic brain injury, adolescence, fMRI, DTI, connectivity, Kaempferol

Running title: Kaempferol treatment after TBI and MRI at adolescence

Table of contents title: MRI at adolescence after traumatic brain injury treatment with Kaempferol

***Correspondence:**

Sridhar Kannurpatti, PhD

Department of Radiology

RUTGERS-New Jersey Medical School

ADMC-5 Room 575

30 Bergen Street, Newark, New Jersey 07103

Phone: 1-(973) 972-7417; Fax: 1-(973) 972-7363

Email: kannursr@njms.rutgers.edu

Abstract

Targeting mitochondrial ion homeostasis using Kaempferol, a mitochondrial Ca^{2+} uniporter channel activator, improves energy metabolism and behavior soon after a traumatic brain injury (TBI) in developing rats. Due to broad TBI pathophysiology and brain mitochondrial heterogeneity, Kaempferol mediated early-stage behavioral and brain metabolic benefits may accrue from diverse sources within the brain. We hypothesized that Kaempferol influences TBI outcome by differentially impacting the neural, vascular and synaptic/axonal compartments. Following TBI at early development (P31), fMRI and DTI were applied to determine imaging outcomes at adolescence (2-months post-injury). Vehicle and Kaempferol treatments were made at 1, 24 and 48 hrs post-TBI and their effects were assessed at adolescence. A significant increase in neural connectivity was observed after Kaempferol treatment as assessed by the spatial extent and strength of the somatosensory cortical and hippocampal RSFC networks. However, no significant RSFC changes were observed in the thalamus. DTI measures of fractional anisotropy (FA) and apparent diffusion coefficient (ADC), representing synaptic/axonal and microstructural integrity, showed significant improvements after Kaempferol treatment, with highest changes in the frontal and parietal cortices and hippocampus. Kaempferol treatment also increased corpus callosal FA, indicating measurable improvement in the inter-hemispheric structural connectivity. TBI prognosis was significantly altered at adolescence by early Kaempferol treatment, with improved neural connectivity, neurovascular coupling and parenchymal microstructure in select brain regions. However, Kaempferol failed to improve vasomotive function across the whole brain, as measured by cerebrovascular reactivity (CVR). The differential effects of Kaempferol treatment on various brain functional compartments support diverse cellular-level mitochondrial functional outcomes in vivo.

Introduction

A large inter-dependence exists between neural circuit activity, the cerebrovascular supply supporting circuit function and synaptic/axonal microstructure, which act in concert to determine systemic sensorimotor and cognitive outcomes. Traumatic brain injury (TBI) pathology is broad, affecting multiple cellular types and hence different neurophysiological variables¹. TBI leads to an energy metabolic decline in pediatric patients and developmental preclinical models of injury,²⁻⁷ consequently affecting downstream function in various cellular compartments.¹ Hence mitochondria, the subcellular organelles responsible for oxidative energy metabolism, and enriched in diverse cell types of the brain are effective targets for TBI treatments. It can be hypothesized that treatments targeting mitochondria can promote diverse cell-type specific downstream repair mechanisms in neurons, glia, vascular smooth muscle and endothelium, which can synergistically improve neurophysiological outcomes. Since energy metabolism is upstream to various cellular processes during recovery from TBI, treatments maintaining mitochondrial ion homeostasis, and hence their energy metabolic capacity, may differentially impact injury prognosis depending on the mitochondrial properties of each brain compartment.

Preservation of energy metabolism in the developing brain is not only crucial for efficient post-TBI repair via downstream energy-dependent mechanisms, but also to sustain normal ongoing developmental changes. Since cerebral vasculature, neural and axonal/synaptic microstructures dynamically change during development,⁸⁻¹² TBI in children are more devastating due to impediments of ongoing normal development. Given the temporally variable characteristics of TBI pathology¹, preclinical experiments reporting on multiple biomarkers of brain function during development, preferably in a simultaneous manner and translatable to humans are necessary. Addressing this gap, our previous study utilized magnetic resonance imaging (MRI) based functional MRI (fMRI) and diffusion tensor imaging (DTI) modalities to simultaneously determine brain structural and functional changes at adolescence after TBI using the development rat model.¹³ The multimodal MRI biomarkers obtained at the adolescent stage strongly correlated with the metabolic decline, reduced neural viability and behavioral debilitation observed during the

early acute/subacute stage (0-72 hours) after TBI.² Acutely targeting mitochondrial ion homeostasis using Kaempferol, a pharmacological enhancer of mitochondrial Ca^{2+} uniporter channel (mCU) activity and hence mitochondrial Ca^{2+} cycling^{14,15}, mitigated the TBI-induced early energy metabolic decline and improved behavioral performance.¹⁶ The early-window Kaempferol treatment regimen (1mg/Kg i.p) at 1, 24 and 48 hrs post-TBI, also improved prognosis at adolescence revealed by better stimulus-induced neurovascular coupling responses and sensorimotor behavior¹⁷.

Using a translatable experimental design and clinically relevant imaging markers, the present study tested the hypothesis that Kaempferol-mediated effects on the brain are diverse, through its variable effects on mitochondria in different cellular types. Rats (age; P31) underwent a fluid percussion TBI in the mild to moderate intensity and randomly assigned to vehicle or Kaempferol (1mg/Kg) groups, where treatments were made at 1, 24 and 48 hours after injury. Using fMRI and DTI measures at adolescence (2 months after injury), various system level biomarkers informing on the neural, vascular and synaptic/axonal compartments were determined to assess TBI prognosis and the effects of Kaempferol treatment.

Materials and Methods

Animals and treatment

Male Sprague-Dawley rats (n=16; 23-24 days old; weighing 60-80g) were procured from Charles River Laboratories, Wilmington, MA, USA and housed in pairs under controlled conditions. All experimental on animals were carried out in accordance with the protocol approved by a local Institutional Animal Care and Use Committee (IACUC) of Rutgers Biomedical and Health Sciences-New Jersey Medical School and Yale University School of Medicine. Kaempferol used in the current study was of commercial grade (Sigma-Aldrich, USA) and freshly prepared into working solution using sterile saline. Routes of administration for vehicle (10% dimethyl sulfoxide in saline) and Kaempferol were through intraperitoneal injection.

Lateral fluid-percussion injury

Rats (age; P31) were subject to lateral fluid percussion injury (FPI) as previously described.^{18,19} The developmental rat age at P31 approximately correspond between 2-4

years of human age,²⁰ The FPI method produced diffuse moderate TBI, very similar to that observed in humans. Briefly, animals were anesthetized with Ketamine (80mg/kg i.p)-Xylazine (10mg/kg i.p) and positioned on a stereotaxic frame after confirming surgical plane anesthesia. A 3mm craniotomy was performed on the left side of the skull -5 mm posterior to the bregma and 3 mm lateral to the sagittal suture while retaining the dura. A Luer-Lock syringe hub was attached surrounding the exposed dura using cyanoacrylate adhesive. 24 hours after the Luer Lock placement, TBI was induced by attaching the Luer-Lock hub of each isoflurane-anesthetized animal to the FPI device (Virginia Commonwealth University, VA, USA). A pendulum drop delivered a brief 20ms impact on the intact dura. The impact pressure was measured by an extra-cranial transducer and controlled between 1.8-2.0 atm. All surgical and experimental conditions in the current treatment groups were kept similar to our prior sham and untreated TBI study for consistency, and which has been published recently¹³. Immediate neurological parameters observation after injury did not lead to any seizure like behavior in all injured animals. Vehicle and Kaempferol treated-TBI animals were monitored within their cage environment on a daily basis. Mortality was observed in two vehicle-treated and one Kaempferol treated animal within 3 days post injury. Surviving animal groups ie., TBI+vehicle (n=5) and TBI+Kaempferol treatment (n=8) underwent the fMRI and DTI measurements for the present study.

Magnetic Resonance Imaging (MRI)

MRI experiments were performed at adolescence (2-months after TBI), translating to approximately 12-14 years of human age.^{20,21} Animals were anesthetized using intraperitoneal injection of urethane (1.3 mg/kg body weight). Tracheostomy was performed on animals to administer a mixture of O₂ and N₂O (30/70%) through a breathing tube. Animals were then placed into a custom-built frame and fixed to ear-bars to minimize motion and produce consistent spatial positioning within the RF coil. Body temperature was monitored throughout the procedure using a rectal probe and maintained within 35-37°C using warm water circulated pad. Chronology of anatomical MRI, functional MRI and Diffusion MRI measures were randomly varied across animal subjects, except the hypercapnic (CO₂) stimulation experiments, which was always performed last.

Anatomical MRI:

MRI scanning was performed on a modified 9.4T system with Bruker spectrometer and custom built ^1H ellipsoidal surface coil (5 x 3 cm). MR-images were acquired over 12 contiguous coronal slices (thickness = 1mm), covering the parenchyma between the olfactory bulb and cerebellum, with an in-plane field of view of 3.2 x 2.4 cm. Anatomical reference images (TR/TE = 4000/30 ms, 2 averages) were acquired in a 128 x 96 matrix, using a RARE sequence providing an in-plane resolution of 250 x 250 μm . Additionally, a fast 3D anatomical scan (TR/TE = 50/5.6 ms, FA = 20°, 2 averages) was acquired with an isotropic resolution of 250 μm , for image registration purposes.

Diffusion MRI:

Diffusion sensitive images for DTI (TR/TE = 4000/20 ms, 4 averages) was acquired as a 4-segment EPI in a 64 x 48 matrix (in-plane resolution = 500 x 500 μm), with 5 A_0 images, 15 diffusion directions and a b-value of 1000 s/mm^2 .

Resting state and cerebrovascular reactivity fMRI:

Resting state and cerebrovascular reactivity fMRI were performed using the gradient echo (GE) echo planar imaging (EPI) sequence (TR/TE= 1000/15 ms, preceded by 8 dummy scans) using the same geometry as diffusion scans (64 x 48 matrix, 500 x 500 μm in-plane resolution) with the GE-EPI sequence producing image contrast sensitive to blood oxygenation changes (BOLD).²² Resting-state fMRI paradigm consisted of a 5 min scan (300 repetitions), acquired in four experimental trials per animal. Cerebrovascular reactivity fMRI scans were obtained using similar GE-EPI parameters as the resting state fMRI which lasted for 12 minutes (720 repetitions). A 10% carbon dioxide gas (CO_2) added to the breathing gas mixture of O_2 and N_2O (30/70%) between minutes 3 and 6 of the acquisition and repeated twice per animal.

Data analysis and statistics:

All EPI images were linearly registered to the subject's native anatomical space before further processing. BioImage Suite software (<http://bioimagesuite.yale.edu/>) was used for the tensor model fitting on a voxel-wise basis using the diffusion sensitive images. Parametric maps of fractional anisotropy (FA) and mean diffusivity (MD) value maps were

obtain as described in our earlier studies.²³ Blood oxygen level dependent (BOLD) fMRI temporal EPI data sets obtained during the resting state and CO₂ challenge experiments were analyzed using the AFNI software.²⁴ EPIs were corrected for slice-time using 3dTshift and motion using 3dvolreg with the 5th sub-brick as the base. EPIs were subsequently spatially smoothed using a Gaussian filter (FWHM = 1.5 mm) and linearly detrended to remove temporal signal drifts for resting-state scans only. No detrending was performed on the CO₂ scans to avoid biasing the BOLD response curve to the single event CO₂ challenge. Our previous quality control scans with the same sequence showed no significant linear drift within 12 minutes the typical length of one CO₂ challenge acquisition. Parametric maps of CO₂ challenge-induced cerebrovascular reactivity were generated from a voxel-level linear model based on the “ON” and “OFF” timing of CO₂ gas delivery and expressed as the *t*-statistical value of the contrast between baseline (Frames 1 to 180) and CO₂ challenge (Frames 210 to 360).

For resting-state functional connectivity (RSFC) analysis, preprocessed EPIs were band pass filtered (0.01 to 0.15 Hz). Six seed voxels were chosen from each region of interest (ROI) from the right hemisphere (contralateral to the injury). The ROIs were somatosensory cortex, hippocampus and thalamic regions ensuring that the seed voxels randomly identified always lie within these respective ROIs identified using the rat brain atlas.²⁵ Signal time series from each selected seed voxel was cross correlated with the entire brain, producing 6 cross-correlation maps for each experimental trial. As demonstrated in our earlier studies in normal²⁶ and TBI animals,¹³ the average RSFC map obtained from the six different cross-correlation maps represented a more accurate topology of the RSFC network. In a similar manner, the 6 correlation maps obtained using 6 random seed voxels within each respective ROI (somatosensory cortical, hippocampus and thalamus) were obtained for each resting state scan leading to 18 correlation maps for 3 experimental trials performed on each animal. Subsequently all correlation maps were averaged across trials and animals in each group. A Fisher *z*-transformation was used to convert the correlation coefficients to *z*-scores before averaging. After averaging, an inverse transform was subsequently used to obtain voxel-wise average correlation coefficient values in the group RSFC maps.

For group statistical comparisons, 3D anatomical images were used to generate a non-linear transform from each animal subject's native space to a common space, consisting of an averaged brain from 8 sham animals obtained from our earlier analysis of sham animals¹³. Since a small ipsilateral distortion occurred along the skull and parenchymal area (injury epicenter) where a fluid percussion Luer Lock existed to enable the fluid percussion traumatic brain injury a non-linear registration was used for the final statistical parameters. Registered anatomy from each animal subject was visually inspected for alignment by overlaying the registered images on the average-sham anatomical MRI template. Subsequently the respective transforms were applied to all parametric maps of FA, ADC, CVR and RSFC networks obtained from all TBI animals (both vehicle and Kaempferol-treated). Regions of interest (ROIs) included the cortex, hippocampus, thalamus, hypothalamus, amygdala and white matter areas such as the corpus callosum, internal capsule and cingulum. ROIs were drawn on the co-registered average sham brain using the rat brain atlas,²⁵ and used across each co-registered individual brain (**Supplementary Figure S1**). Similar to our earlier analyses of the sham and untreated-TBI groups,¹³ the cortical ROIs encompassed motor, somatosensory, parietal, auditory, visual, perirhinal and entorhinal areas for consistent comparisons (**Supplementary Figure S1**). For each modality, group differences were calculated using a voxel level general linear model (t distribution), with treatment as the contrast and standard deviation calculated at each voxel. Significance was defined as a threshold of $p < 0.05$ after correcting for multiple comparisons using a random field theory approach, accounting for the cluster size of contiguous significant voxels.²⁷

Results

Multimodality imaging with DTI-based fractional anisotropy (FA) and apparent diffusion coefficient (ADC) variables were used as markers of brain parenchymal changes, which is known to correlate with synaptic/axonal microstructure. fMRI-BOLD based resting state functional connectivity (RSFC) was used as a marker of neural circuit activity and transient hypercapnia-induced fMRI-BOLD as a surrogate for cerebrovascular reactivity (CVR). Together these parameters provide a multidimensional assessment of the effects of Kaempferol treatment in improving outcomes of developmental TBI.

In our prior studies, comparison of DTI responses between sham and TBI groups revealed a significant reduction in FA and increased ADC, spreading bilaterally and across the inter-hemispheric white matter regions such as the corpus callosum.¹³ Specifically, bilateral FA decreases were observed in the somatosensory and entorhinal cortices, whereas unilateral FA decreases were prominent in the ipsilateral cingulum and internal capsule regions of interest (ROIs).¹³ ADC values between sham and TBI in our previous studies increased significantly in the same ROIs, indicating increased isotropic diffusion after TBI and consistent with the decreased FA.¹³ In the current study comparing Kaempferol and vehicle treatments in TBI animals, strong unilateral and bilateral increases in FA occurred after Kaempferol treatment when compared to vehicle (**Figure 1A**). As observed by the group statistical maps of vehicle vs Kaempferol, FA increases were mostly across the peri-lesional regions away from the injury epicenter (**Figure 1A**). Unilateral FA increases were observed within the ipsilateral perirhinal cortex, hippocampus, hypothalamus, thalamus and amygdala, whereas bilateral FA increases were observed across motor, somatosensory cortices, insula and caudate putamen (**Figure 1A**). FA increase with Kaempferol treatment across various anatomical regions statistically determined in **Figure 1A** are depicted in the supplementary **Figure S2B**. Significant Kaempferol-induced microstructural integrity improvement as determined by increased FA was observed in various white matter ROIs, including the corpus callosum and across both hemispheres in the cingulum and internal capsule (**Figure 1B**). ADC values decreased after Kaempferol treatment compared to vehicle. Although ADC decreases were relatively sparse compared to FA, the group statistical maps indicated highly specific ADC decreases across ipsilateral cortical regions, hippocampus, internal capsule and bilaterally across the hypothalamus (**Figure 1C**). ADC changes determined across different white matter ROIs showed significant ADC decrease only across the corpus callosum after Kaempferol treatment when compared to vehicle (**Figure 1D**). ADC decrease after Kaempferol treatment across various anatomical regions statistically determined in **Figure 1B** are depicted in the supplementary **Figure S2D**. Taken together with our prior results of untreated TBI versus sham¹³, the current DTI results after treatment highlights the protective effect of Kaempferol not only in the most vulnerable regions after TBI such as

the perirhinal cortex, hippocampus, hypothalamus, thalamus, amygdala, and corpus callosum, but also across additional structures such as the insula and caudate putamen.

From our previous studies, all RSFC networks (somatosensory cortical, hippocampal and thalamic seed voxels) were observed to have higher bilateral symmetry in sham compared to TBI animals. A significant ipsilateral decrease in RSFC network spatial extent was observed in TBI when compared to sham.¹³ In the current treatment study, all RSFC networks (somatosensory cortical, hippocampal and thalamic) showed similar ipsilateral RSFC spatial extent decrease in the vehicle-treated TBI animal group (**Figures 2A,3A and 4A**), and comparable to the untreated TBI group observed earlier¹³. Kaempferol's effect on RSFC was investigated by comparing the vehicle- and Kaempferol treated TBI groups across the somatosensory cortical, hippocampal and thalamic RSFC networks. A significant bilateral increase in RSFC network spatial extent occurred across the cortical and hippocampal networks (**Figure 2A and 3A**), whereas no significant changes were apparent in the thalamic RSFC network (**Figure 4A**). RSFC strength in various anatomical ROIs within these RSFC networks, have been shown previously to decrease after TBI when compared to sham.¹³ RSFC strength was estimated from the frontal and parietal cortical, hippocampal and thalamic ROIs from the vehicle and Kaempferol-treated TBI groups. Kaempferol treatment led to significant increases in RSFC strength when compared to vehicle over multiple anatomical ROIs spanned by the somatosensory cortical RSFC network (**Figures 2B**). A similar Kaempferol-induced increase in RSFC strength was observed across multiple ROIs spanned by the hippocampal RSFC network (**Figures 3B**). As observed by the relatively larger statistical clusters in the ipsilateral hemisphere adjoining the injury site between vehicle and Kaempferol treated TBI animal groups (arrows; **Figures 2C and 3C**), Kaempferol was found to reduce the inter-hemispheric asymmetry in the somatosensory cortical and hippocampal RSFC networks.

fMRI measures of cerebrovascular reactivity (CVR) were obtained using a transient (3 min) inhalation of 10% CO₂ gas mixture to induce hypercapnia as a vasodilatory stimulus. CVR maps, reporting on regional vasomotive functions were obtained on a voxel-wise manner basis based on fMRI-BOLD response amplitude to the CO₂ stimulus as assessed by our previous studies.¹³ While sham animals had a significantly higher global CVR

compared to untreated-TBI as assessed by our previous studies,¹³ the current results assessing Kaempferol effects against TBI showed no significant effect on the CVR when compared to vehicle-treated TBI animals (**Figure 5**). Quantitative statistical comparisons using a t-test between vehicle and Kaempferol groups, performed voxel-wise throughout the brain, did not reveal any significant clusters of altered CVR (data not shown).

Discussion

Kaempferol dose used in the present study was in the range of human dietary intake of flavonol rich foods²⁸ and 1000 times lower than the human safety limits of 1000 mg/Kg.²⁹ No significant differences were observed in mortality between vehicle and Kaempferol treated TBI animals. As a natural flavonoid compound, Kaempferol has been shown to specifically act on the mitochondrial Ca^{2+} uniporter (mCU) channel by enhancing its activity *in vitro*,¹⁴ and capable of crossing the blood brain barrier.³⁰ Low-dose acute Kaempferol treatments *in vivo* (ie., 1mg/Kg i.v) have demonstrated its neuroactive effects of boosting stimulus-induced neurovascular coupling,^{31,32} neuronal electrical activity and the baseline oxidative metabolism in the normal brain.³² Studying Kaempferol's mechanism of action *in vivo*, comparable doses of 1mg/Kg i.p Kaempferol treatments were made during the acute/subacute window (1, 24 and 48 hours post-TBI) and assessed *in vivo* using the rat model of developmental TBI.¹⁶ This early Kaempferol treatment mitigated the TBI-induced brain energy metabolic decline, improved neural viability and behavior at 72 hours post injury.¹⁶ A metabolome-wide analysis of the brain indicated that Kaempferol's effects in the post-TBI brain was predominantly via its action on mitochondria-related biochemical pathways.¹⁶ Kaempferol's mitochondrially-mediated effects including early bioenergetic stress mitigation after TBI, significantly altered the trajectory of developmental TBI at adolescence. Such a long-term beneficial effect on TBI prognosis was supported by our Kaempferol treatment studies, which improved behavioral and stimulation-induced cerebral blood flow (CBF) responses at adolescence (2 months after TBI).¹⁷

Mitochondrial heterogeneity and the hypothesis of differential treatment outcomes across brain compartments and regions.

While the *in vivo* treatment studies have so far established Kaempferol's mitochondrial mechanism of action, neuroactive impact in the working brain and beneficial effects in developmental TBI outcomes,^{16,31-33} its overall systemic impact within the brain can be hypothesized to vary depending on mitochondrial structural and functional heterogeneity across various cellular populations. Brain regional mitochondrial heterogeneity and its placement within the context of cellular, functional, developmental and neuroanatomical environment are crucial to interpret pediatric brain pathophysiological changes. Additionally active consideration of mitochondrial heterogeneity, which is the true *in vivo* scenario, may help reconcile the differential impact of mitochondrially targeted treatments across various brain compartments.³⁴ Hence Kaempferol-induced mitochondrial functional changes and its consequent downstream impact on cellular pathways was hypothesized to manifest in a heterogeneous manner in a variety of cellular populations. The current multimodal imaging design with clinically relevant markers enabled testing across cellular compartments and brain regions. Different multimodal imaging outcome results demonstrate the heterogeneous impact of mitochondrially targeted Kaempferol treatment across different cell types of the brain *in vivo*.

Neuronal (synaptic/non-synaptic) and astroglial mitochondrial impact³⁵

RSFC topology was significantly improved across the somatosensory cortical and hippocampal but not thalamic networks after Kaempferol treatments signifying a favorable outcome on the neuronal mitochondrial compartments (**Figures 2,3 and 4**). Both synaptic and non-synaptic mitochondria seem to be affected as observed from the increases in FA (**Figure 1A and 1B**) and somatosensory cortical RSFC network topology and strength (**Figure 2**). Earlier studies with the same dose of Kaempferol showed improved stimulation-induced cerebral blood flow (CBF) responses, suggesting improved neural circuit activity and neurovascular coupling.¹⁷ As astrocytes significantly enable the neurovascular coupling process, their mitochondria are likely to have been impacted

leading to better astrocytic Ca^{2+} signaling and neurovascular activity. As Ca^{2+} overload occurs in the temporal window of approximately 6 hours after TBI through mitochondrial dysfunction and arrest of Ca^{2+} transport,³⁶ the ion homeostatic benefits derived by both neuronal and astroglial mitochondria from Kaempferol treatment to improve their viability and function. However, the intensity of Kaempferol action is likely to vary depending on the functional differences of neuronal and astroglial mitochondria. Even across neurons, both synaptic and non-synaptic mitochondria may derive different Kaempferol treatment benefits with synaptic mitochondria receiving a higher impact. This possibility is due to a relatively greater TBI-induced oxidative damage of synaptic mitochondria when compared to non-synaptic.³⁵ Further heterogeneous effects could be observed in the thalamic RSFC network which showed no significant impact of Kaempferol (**Figure 4**), contrasting the robust neural connectivity improvements within the somatosensory cortical (**Figure 2**) and hippocampal RSFC networks (**Figure 3**).

Although the thalamic region is very functionally diverse containing several nuclei with specific functions, the individual thalamic RSFC networks obtained from the six seed voxels placed randomly in different locations within the thalamic ROI has been shown to be topologically stable as demonstrated our earlier study.²⁶ Hence spatially separated selection of the 6 random seed voxels within all ROIs, including the thalamic ROI, was unlikely to cause any significant RSFC variability resulting in no improvement of thalamic RSFC after Kaempferol treatment. Thalamic regions also do not display neurodegeneration, but show gradual neuronal atrophy from early perisomatic axotomy after a diffuse brain injury, very similar to our current model.³⁷ The subsequent post-TBI reorganization of the thalamus is also complex, leading to hypersensitivity in somatosensory responses and hypothesized as a maladaptive reorganization extending into the chronic time periods after TBI.³⁸ A diminishing RSFC spatial extent and strength in the ipsilateral thalamic regions at adolescence corroborate prior neuronal atrophic evidence.³⁷ However, Kaempferol's inability to improve thalamic RSFC strength, in the current study, may point to a differently vulnerable mitochondrial population supporting a prolonged neural atrophic mechanism.

Endothelial and smooth muscle mitochondria impact^{39,40}

Extracellular mitochondria after a central nervous system (CNS) injury have been proposed as a cellular rescue signal⁴¹, and demonstrated to improve endothelial function *in vivo* after a stroke.⁴² Although endothelial mitochondrial properties can be expected to differ from neural mitochondria in certain specific functions, they would generally benefit from Kaempferol treatment since the mitochondrial Ca^{2+} uniporter channel (mCU), which is the target for Kaempferol is expressed in all mitochondrial types. While it is not known if mCU densities varied across various distinct cellular mitochondria within the CNS, enhanced survival capability of extracellular endothelial mitochondria from damaged vasculature can potentially alter the overall endothelial population responses post TBI in a beneficial direction. Supporting this view, improved stimulation-induced neurovascular activity after TBI suggest that the capillaries of the neurovascular units functioned better after Kaempferol treatment¹⁷. However, no significant improvement was observed in CVR in response to a transient hypercapnic challenge, which predominantly tests the functionality of large and intermediate cerebral arteries^{43,44}. The current result infers that smooth muscle mitochondria and hence their function was the least affected by Kaempferol treatment. Supporting this result, regional baseline CBF perfusion deficits after TBI, stemming from mostly large and intermediate vessel disruptions after injury, were observed to persist through development in the current model of TBI.¹⁷ Kaempferol treatment, although helpful in improving behavioral and brain responses, had no effect on the decreased baseline CBF perfusion observed ipsilateral to the TBI.¹⁷ Decreased CBF is a hallmark of concussive TBI in humans.⁴⁵ and its acute vascular origins and cellular mechanisms have been well studied in preclinical animal models of TBI of various severity.⁴⁶ While chronic vascular rearrangement continues beyond 6 months after TBI with significant vessel proliferation in both the lesional and perilesional regions, there are no direct correlation between CBF and regenerated vessel density.⁴⁷ Furthermore, prolonged inflammation, BBB disruption and white matter damage may sustain chronic microvascular dysfunctions after TBI.⁴⁸ Recent studies indicate impaired myogenic constriction of cerebral arteries through mitochondrial oxidative stress after a TBI, which was restored by mitoTEMPO, a mitochondria-targeted antioxidant.⁴⁹ Hence TBI-induced mitochondrial

responses maybe very different in vascular cells, necessitating entirely different doses of Kaempferol for optimal effects. Higher doses of Kaempferol is known to induce significant antioxidative and anti-inflammatory responses. Hence, future dose escalation studies may help determine possibilities of cerebrovascular protection through mitochondrially triggered redox- and immuno-modulations.

To determine vehicle effects within the brain, untreated and vehicle-treated TBI animal comparisons were made in our earlier study, which showed no significant vehicle-induced effects on the brain metabolome.² Hence vehicle treated sham group was not considered in the current study. Furthermore, given Kaempferol's properties as a dietary flavonol compound with proven safety in humans,²⁸ it is highly unlikely that Kaempferol may have significant effects on the structural or functional components within the normal working brain. Hence the absence of a Kaempferol-treated sham group in the current study, although a moderate weakness, is very unlikely to alter the overall conclusion of the study.

Conclusion

As TBI pathology is broad, its prognosis and treatment outcomes can be best understood multi-dimensionally using a systems approach spanning the genomic, proteomic, metabolomic, tissue, organ and organism levels.⁵⁰ The demonstrated multimodal translational imaging of TBI treatment and its ability to distinguish mitochondrial treatment responses across various tissue compartments and regions indicates its critical value within this futuristic systems framework. While the Kaempferol dose used in the current preclinical trial favorably impacted neural populations, a lack of cerebrovascular improvement and minimal neural impact in the thalamic region indicated mitochondrial functional diversity. The current results justify future Kaempferol dose/treatment window optimizations extending to cerebrovascular protection, with potential to further enhance the improved behavioral and brain responses after TBI.

Disclosure statement: All authors disclose that no competing financial interests exist

Acknowledgements: Funding from the New Jersey Commission for Brain Injury research CBIR15IRG010 (SK), R01 NS097750 (VS), R01 MH067528 (FH) and P30 NS052519 (FH) are acknowledged.

References

- 1 Park, E., Bell, J. D., Baker, A. J. (2008). Traumatic brain injury: Can the consequences be stopped? *Can Med Assoc J* 178, 1163-1170.
- 2 Chitturi, J., Li, Y., Santhakumar, V., Kannurpatti, S.S. (2018). Early behavioral and metabolomic change after mild to moderate traumatic brain injury in the developing brain. *Neurochem Int* 120, 75-86.
- 3 Prins, M.L. (2017). Glucose metabolism in pediatric traumatic brain injury. *Child's nervous system : ChNS :official journal of the International Society for Pediatric Neurosurgery* 33, 1711-1718.
- 4 Robertson, C. L. Saraswati, M., Scafidi, S., Fiskum, G., Casey, P., McKenna, M. (2013). Cerebral Glucose Metabolism in an Immature Rat Model of Pediatric Traumatic Brain Injury. *J Neurotrauma* 30, 2066-2071.
- 5 Casey, P., McKenna, M., Saraswati, M., Robertson, C., Fiskum, G. (2006). Traumatic brain injury in immature rats causes early and sustained alterations in cerebral metabolism. *Crit Care Med* 34, A17-A17.
- 6 Marino, S. Zei, E., Battaglini, M., Vittori, C., Buscalferri, A., Bramanti, P., Federico, A., De Stefano, N. (2007). Acute metabolic brain changes following traumatic brain injury and their relevance to clinical severity and outcome. *J Neurol Neurosurg Psychiatry* 78, 501-507.
- 7 Ragan, D.K., McKinstry, R., Benzinger, T., Leonard, J.R., Pineda, J.A. (2013). Alterations in cerebral oxygen metabolism after traumatic brain injury in children. *J Cereb Blood Flow Metab* 33, 48-52.
- 8 Biagi, L. Abbruzzese, A., Bianchi, M.C., Alsop, D.C., Del Guerra, A., Tosetti, M. (2007). Age dependence of cerebral perfusion assessed by magnetic resonance continuous arterial spin labeling. *Journal of magnetic resonance imaging : JMRI* 25, 696-702.
- 9 Chiron, C. Raynaud, C., Maziere, B., Zilbovicius, M., Laflamme, L., Masure, M.C., Dulac, O., Bourguignon, M., Syrota, A. (1992). Changes in regional cerebral blood flow during brain maturation in children and adolescents. *Journal of nuclear medicine : official publication, Society of Nuclear Medicine* 33, 696-703.

- 10 Chugani, H.T., Phelps, M.E., Mazziotta, J.C. (1987). Positron emission tomography study of human brain functional development. *Ann Neurol* 22, 487-497.
- 11 Paus, T. Collins, D.L., Evans, A.C., Leonard, G., Pike, B., Zijdenbos, A. (2001). Maturation of white matter in the human brain: a review of magnetic resonance studies. *Brain Res Bull* 54, 255-266.
- 12 Winter, J.D. Dorner, S., Lukovic, J., Fisher, J.A., St Lawrence, K.S., Kassner, A. (2011). Noninvasive MRI measures of microstructural and cerebrovascular changes during normal swine brain development. *Pediatric research* 69, 418-424.
- 13 Parent, M. Li, Y., Santhakumar, V., Hyder, F., Sanganahalli, B.G., Kannurpatti, S.S. (2018). Alterations of parenchymal microstructure, neuronal connectivity and cerebrovascular resistance at adolescence following mild to moderate traumatic brain injury in early development. *J Neurotrauma* 36, 601-608.
- 14 Montero, M. Lobaton, C. D., Hernandez-Sanmiguel, E., Santodomingo, J., Vay, L., Moreno, A., Alvarez, J. (2004). Direct activation of the mitochondrial calcium uniporter by natural plant flavonoids. *Biochem J* 384, 19-24.
- 15 Vay, L. Hernandez-Sanmiguel, E., Santo-Domingo, J., Lobaton, C. D., Moreno, A., Montero, M., Alvarez, J. (2007). Modulation of Ca(2+) release and Ca(2+) oscillations in HeLa cells and fibroblasts by mitochondrial Ca(2+) uniporter stimulation. *J Physiol* 580, 39-49.
- 16 Chitturi, J., Santhakumar, V., Kannurpatti, S.S. (2019). Beneficial effects of Kaempferol after developmental TBI is through protection of mitochondrial function, oxidative metabolism and neural viability. *J Neurotrauma*. doi: 10.1089/neu.2018.6100. [Epub ahead of print].
- 17 Murugan, M., Santhakumar, V., Kannurpatti, S.S. (2016). Facilitating mitochondrial calcium uptake improves activation-induced cerebral blood flow and behaviour after mTBI. *Frontiers in Neuroscience*, doi: 10.3389/fnsys.2016.00019.
- 18 Gupta, A., Elgammal, F.S., Proddutur, A., Shah, S., Santhakumar, V. (2012). Decrease in tonic inhibition contributes to increase in dentate semilunar granule cell excitability after brain injury. *J Neurosci* 32, 2523-2537.

- 19 Li, Y., Korgaonkar, A.A., Swietek, B., Wang, J., Elgammal, F. S., Elkabes, S., Santhakumar, V. (2015). Toll-like receptor 4 enhancement of non-NMDA synaptic currents increases dentate excitability after brain injury. *Neurobiol Dis* 74, 240-253.
- 20 Clancy, B., Darlington, R. B., Finlay, B. L. Translating developmental time across mammalian species. (2001). *Neuroscience* 105, 7-17.
- 21 Andreollo, N. A., Santos, E. F. d., Araujo, M. R., Lopes, L. R. Rat's age versus human's age: what is the relationship? (2012) *Arq Bras Cir Dig* 25, 49-51.
- 22 Ogawa, S., Lee, T. M., Nayak, A. S., Glynn, P. (1990). Oxygenation-sensitive contrast in magnetic resonance image of rodent brain at high magnetic fields. *Magn Reson Med* 14, 68-78.
- 23 Kaneko, G. Sanganahalli, B. G., Groman, S. M., Wang, H., Coman, D., Rao, J., Herman, P., Jiang, L., Rich, K., de Graaf, R. A., Taylor, J. R., Hyder, F. (2017). Hypofrontality and Posterior Hyperactivity in Early Schizophrenia: Imaging and Behavior in a Preclinical Model. *Biol Psychiat* 81, 503-513.
- 24 Cox, R.W. (1996). AFNI: software for analysis and visualization of functional magnetic resonance neuroimages. *Comput Biomed Res* 29, 162-173.
- 25 Paxinos, G., Watson, C. (1998). The rat brain in stereotaxic coordinates. 4th edn, Academic Press.
- 26 Sanganahalli, B. G., Herman, P., Hyder, F., Kannurpatti, S.S. Mitochondrial functional state impacts spontaneous neocortical activity and resting state fMRI.(2013) *PLoS One* 8, e63317, doi:10.1371/journal.pone.0063317PONE-D-13-01544.
- 27 Worsley, K. J. Marrett, S., Neelin, P., Vandal, A.C., Friston, K.J., Evans, A.C. (1996). A unified statistical approach for determining significant signals in images of cerebral activation. *Hum Brain Mapp* 4, 58-73.
28. DuPont, M.S., Day, A.J., Bennett, R.N., Mellon, F.A., Kroon, P.A. (2004). Absorption of kaempferol from endive, a source of kaempferol-3-glucuronide, in humans. *Eur J Clin Nutr* 58, 947-954.
- 29 Shih, T.Y., Young, T. H., Lee, H.S., Hsieh, C.B., Hu, O.Y. (2013). Protective effects of kaempferol on isoniazid- and rifampicin-induced hepatotoxicity. *AAPS J* 15, 753-762.

- 30 Liu, R., Wang, X., Zhao, Y., Wang, Z., Du, L. (2006). The uptake behaviors of kaempferol and quercetin through rat primary cultured cortical neurons. *Biomed Chromatogr* 20, 1178-1184.
- 31 Kannurpatti, S.S., Biswal, B.B. (2008). Mitochondrial Ca²⁺ uniporter blockers influence activation-induced CBF response in the rat somatosensory cortex. *J Cereb Blood Flow Metab* 28, 772-785.
- 32 Sanganahalli, B.G., Herman, P., Hyder, F., Kannurpatti, S.S. (2013). Mitochondrial calcium uptake capacity modulates neocortical excitability. *J Cereb Blood Flow Metab* 33, 1115-1126.
- 33 Kannurpatti, S.S., Sanganahalli, B.G., Herman, P., Hyder, F. (2015). Role of mitochondrial calcium uptake homeostasis in resting state fMRI brain networks. *NMR Biomed* 28, 1579-1588.
- 34 Dubinsky, J.M. (2009). Heterogeneity of nervous system mitochondria: location, location, location! *Exp Neurol* 218, 293-307.
- 35 Hill, R.L., Kulbe, J.R., Singh, I. N., Wang, J.A., Hall, E.D. (2018). Synaptic Mitochondria are More Susceptible to Traumatic Brain Injury-induced Oxidative Damage and Respiratory Dysfunction than Non-synaptic Mitochondria. *Neuroscience* 386, 265-283.
- 36 Xiong, Y., Gu, Q., Peterson, P.L., Muizelaar, J.P., Lee, C.P. (1997). Mitochondrial dysfunction and calcium perturbation induced by traumatic brain injury. *J Neurotrauma* 14, 23-34.
- 37 Lifshitz, J., Kelley, B. J., Povlishock, J. T. (2007). Perisomatic thalamic axotomy after diffuse traumatic brain injury is associated with atrophy rather than cell death. *J Neuropathol Exp Neurol* 66, 218-229.
- 38 Thomas, T. C., Ogle, S.B., Rumney, B.M., May, H.G., Adelson, P.D., Lifshitz, J. (2018). Does time heal all wounds? Experimental diffuse traumatic brain injury results in persisting histopathology in the thalamus. *Behav Brain Res* 340, 137-146.
- 39 Davidson, S.M., Duchon, M.R. (2007). Endothelial mitochondria: contributing to vascular function and disease. *Circ Res* 100, 1128-1141.

- 40 Kluge, M. A., Fetterman, J. L., Vita, J. A. (2013). Mitochondria and endothelial function. *Circ Res* 112, 1171-1188.
- 41 Hayakawa, K. Bruzzese, M., Chou, S.H., Ning, M., Ji, X., Lo, E.H. (2018). Extracellular Mitochondria for Therapy and Diagnosis in Acute Central Nervous System Injury. *JAMA Neurol* 75, 119-122.
- 42 Hayakawa, K. Chan, S.J., Mandeville, E.T., Park, J.H., Bruzzese, M., Montaner, J., Arai, K., Rosell, A., Lo, E. H. (2018). Protective Effects of Endothelial Progenitor Cell-Derived Extracellular Mitochondria in Brain Endothelium. *Stem Cells* 36, 1404-1410.
- 43 Kannurpatti, S.S., Biswal, B.B. (2008). Detection and scaling of task-induced fMRI-BOLD response using resting state fluctuations. *Neuroimage* 40, 1567-1574.
- 44 Kannurpatti, S.S., Biswal, B.B., Hudetz, A.G. (2002). Differential fMRI-BOLD signal response to apnea in humans and anesthetized rats. *Magn Reson Med* 47, 864-870.
- 45 Giza, C.C., Hovda, D.A. (2014). The new neurometabolic cascade of concussion. *Neurosurgery* 75 Suppl 4, S24-33.
- 46 Salehi, A., Zhang, J. H., Obenaus, A. (2017). Response of the cerebral vasculature following traumatic brain injury. *J Cereb Blood Flow Metab* 37, 2320-2339.
- 47 Hayward, N.M. Immonen, R., Tuunanen, P.I., Nde-Ekane, X. E., Grohn, O., Pitkanen, A. (2010). Association of chronic vascular changes with functional outcome after traumatic brain injury in rats. *J Neurotrauma* 27, 2203-2219.
- 48 Glushakova, O. Y., Johnson, D., Hayes, R. L. (2014). Delayed increases in microvascular pathology after experimental traumatic brain injury are associated with prolonged inflammation, blood-brain barrier disruption, and progressive white matter damage. *J Neurotrauma* 31, 1180-1193.
- 49 Szarka, N., Pabbidi, M.R., Amrein, K., Ceziter, E., Berta, G., Pohoczky, K., Helyes, Z., Ungvari, Z., Koller, A., Buki, A., Toth, P. (2018). Traumatic Brain Injury Impairs Myogenic Constriction of Cerebral Arteries: Role of Mitochondria-Derived H₂O₂ and TRPV4-Dependent Activation of BK_{Ca} Channels. *J Neurotrauma*, doi: 10.1089/neu.2017.5056. [Epub ahead of print].
- 50 Fiandaca, M.S. Mapstone, M., Connors, E., Jacobson, M., Monuki, E.S., Malik, S., Macciardi, F., Federoff, H.J. (2017). Systems healthcare: a holistic paradigm for tomorrow. *BMC Syst Biol* 11, 142.

Figure captions

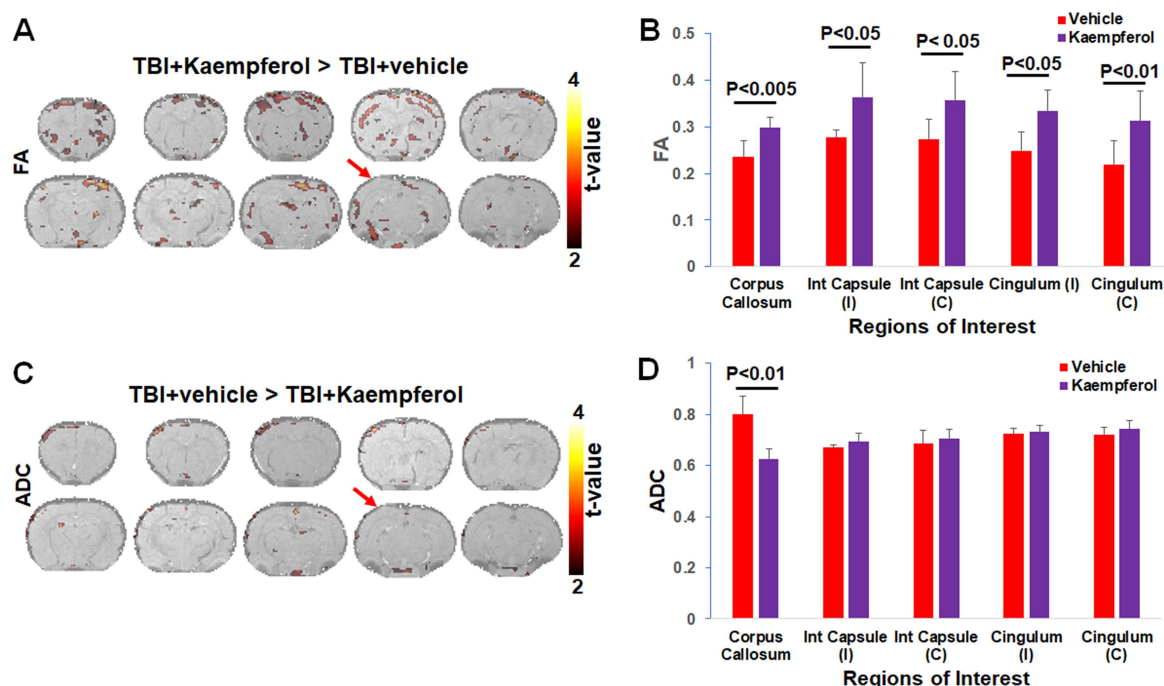


Figure 1. Diffusion tensor imaging (DTI) group average of fractional anisotropy (FA) and apparent diffusion coefficient (ADC) in TBI animals treated with Kaempferol and vehicle. **A.** FA (TBI+Kaempferol>TBI+vehicle), **B.** ADC (TBI+vehicle>TBI+Kaempferol). Significant difference determined by a two-way t-test corrected for multiple comparisons. Voxels with t-values >2; corresponding to a corrected $P<0.05$ are significantly different TBI+Kaempferol vs TBI+vehicle (depicted by color statistical overlay on the rat brain atlas registered anatomical image). ROIs enclosing the corpus callosum, cingulum and internal capsule were used to average voxel-level and group-level parameters of **C.** FA and **D.** ADC. Significant Kaempferol-induced microstructural changes as determined by FA and ADC was observed in the corpus callosum. Cingulum and internal capsule across both hemispheres also showed significant Kaempferol-induced FA changes. Unpaired two-tailed t-test with $P<0.05$ required for significance. Arrows indicate the location of fluid percussion TBI.

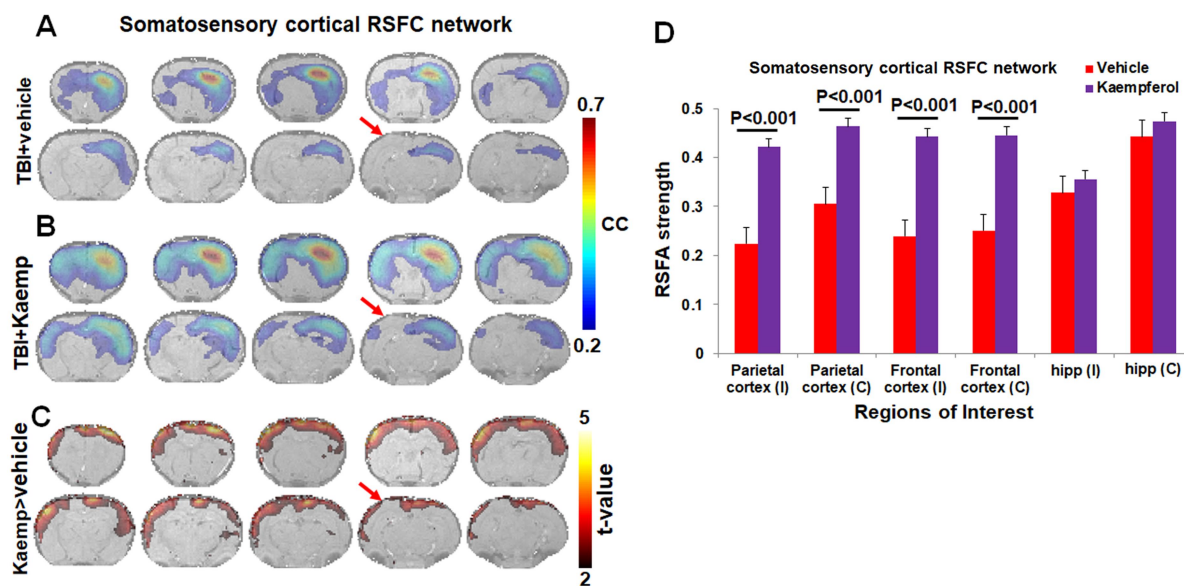


Figure 2. Resting state functional connectivity (RSFC) maps obtained from the vehicle and Kaempferol treated TBI animal groups. Six random seeds from the right somatosensory cortical ROI was used from each subject. Cortical RSFC networks were obtained after cross correlating the seed voxel fMRI-BOLD time series with the signal time series across all voxels in the brain and subsequently averaged across trials and animals within each group after Fisher Z-transform. Voxels with average correlation coefficients (cc) >0.2; corresponding to a corrected $P < 0.05$ represented active voxels of the cortical RSFC network. **A.** TBI+vehicle group, **B.** TBI+Kaempferol group. **C.** Significant difference determined by a two-way t-test corrected for multiple comparisons between TBI+Kaempferol and TBI+vehicle groups. Voxels with t-values >2; corresponding to a corrected $P < 0.05$ are significantly different (depicted by the color statistical overlay on the rat brain atlas registered anatomical image). **D.** RSFC strength determined after averaging the cc values from the frontal and parietal cortical and hippocampal ROIs from either hemisphere in the Kaempferol and vehicle treated TBI groups. Kaempferol (n=8) significantly improved RSFC strength when compared to vehicle (n=5) across all ROIs except hippocampus on both hemispheres. Unpaired two-tailed t-test with $P < 0.05$ required for significance. Arrows indicate the location of fluid percussion TBI.

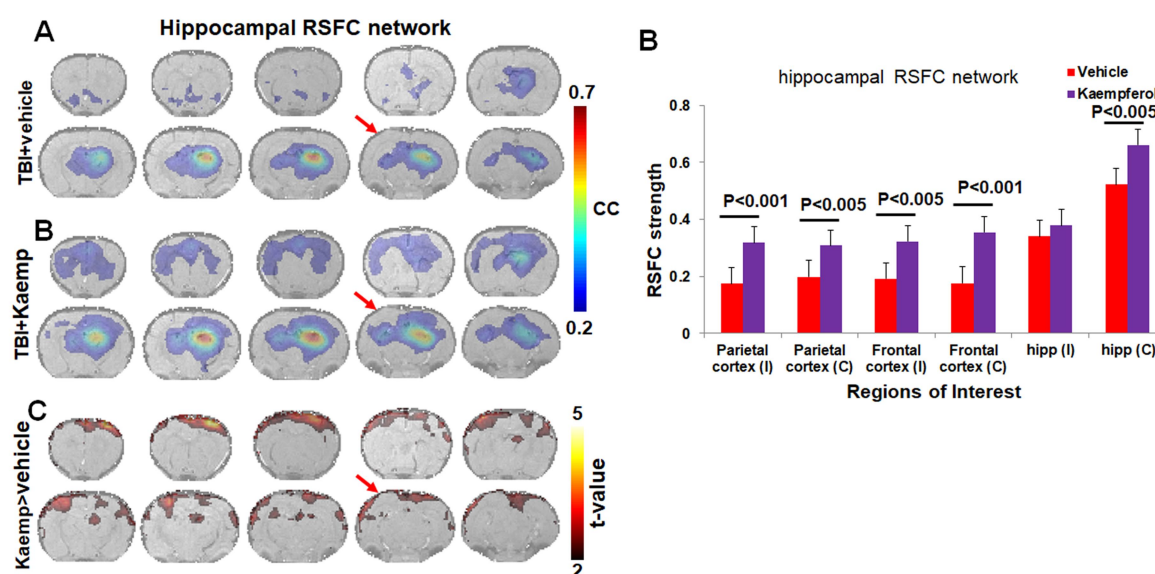


Figure 3. Resting state functional connectivity (RSFC) maps obtained from the vehicle and Kaempferol treated TBI animal groups. Six random seeds from the right hippocampal ROI was used from each subject. Hippocampal RSFC networks were obtained after cross correlating the seed voxel fMRI-BOLD time series with the signal time series across all voxels in the brain and subsequently averaged across trials and animals within each group after Fisher Z-transform. Voxels with average correlation coefficients (cc) >0.2; corresponding to a corrected $P<0.05$ represented active voxels of the hippocampal RSFC network. **A.** TBI+vehicle group, **B.** TBI+Kaempferol group. **C.** Significant difference determined by a two-way t-test corrected for multiple comparisons between TBI+Kaempferol and TBI+vehicle groups. Voxels with t-values >2; corresponding to a corrected $P<0.05$ are significantly different (depicted by the color statistical overlay on the rat brain atlas registered anatomical image). **D.** RSFC strength determined after averaging the cc values from the frontal and parietal cortical and dorsal hippocampal ROIs from either hemisphere in the Kaempferol and vehicle treated TBI groups. Kaempferol ($n=8$) significantly improved RSFC strength when compared to vehicle ($n=5$) in the frontal and parietal cortices across both hemisphere and the contralateral hippocampus. Unpaired two-tailed t-test with $P<0.05$ required for significance. Arrows indicate the location of fluid percussion TBI.

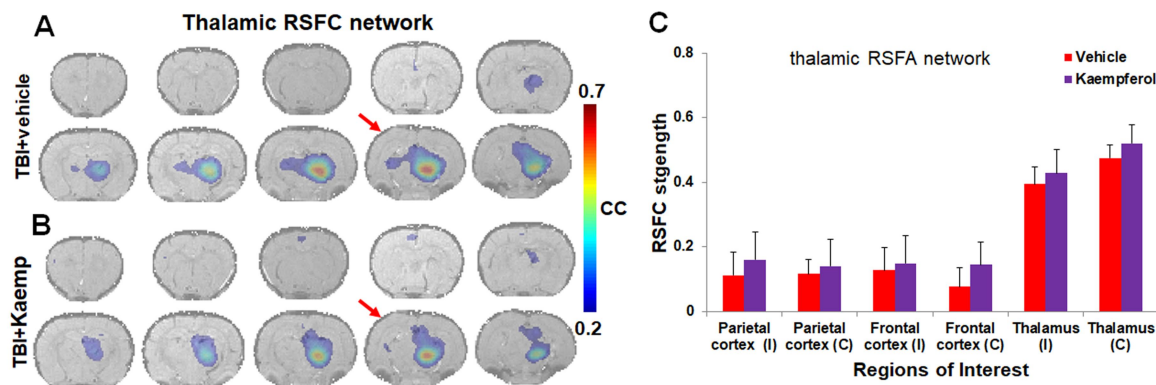


Figure 4. Resting state functional connectivity (RSFC) maps obtained from the vehicle and Kaempferol treated TBI animal groups. Six random seeds from the right thalamic ROI was used from each subject. Thalamic RSFC networks were obtained after cross correlating the seed voxel fMRI-BOLD time series with the signal time series across all voxels in the brain and subsequently averaged across trials and animals within each group after Fisher Z-transform. Voxels with average correlation coefficients (cc) >0.2 ; corresponding to a corrected $P < 0.05$ represented active voxels of the cortical RSFC network. **A.** TBI+vehicle group, **B.** TBI+Kaempferol group. **C.** RSFC strength determined after averaging the cc values from the frontal and parietal cortical and thalamic ROIs from either hemisphere in the Kaempferol and vehicle treated TBI groups. Kaempferol ($n=8$) although with greater average RSFC strength when compared to vehicle ($n=5$) across all ROIs showed no significant differences. Unpaired two-tailed t-test with $P < 0.05$ required for significance. Arrows indicate the location of fluid percussion TBI.

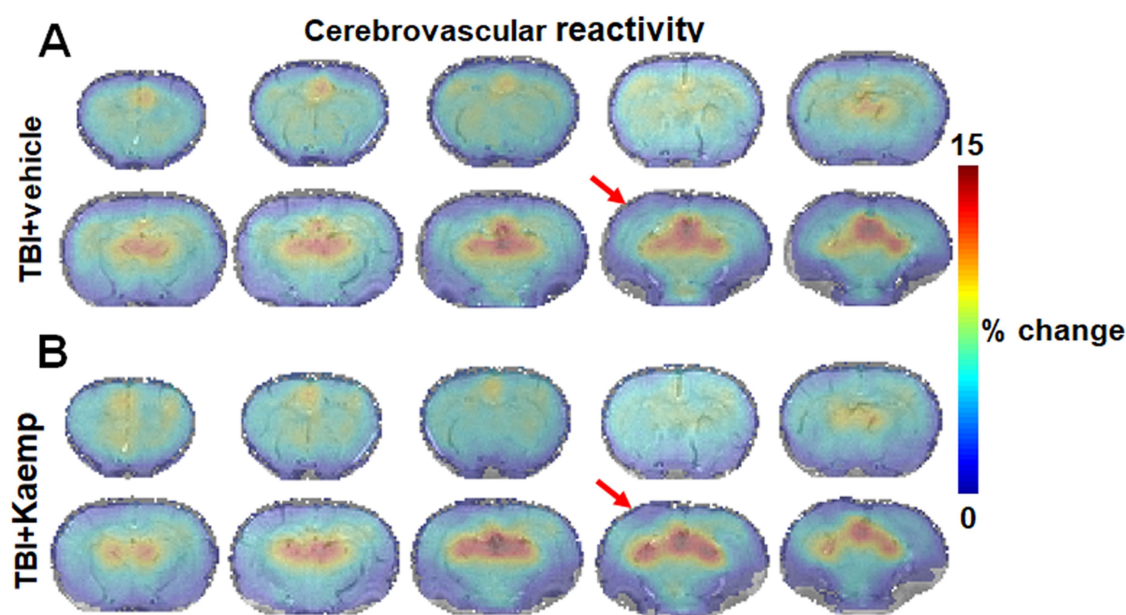


Figure 5. Cerebrovascular reactivity response to transient (10%) carbon dioxide inhalation in **A.** TBI+vehicle (n=5), **B.** TBI+Kaempferol (n=8). Significant difference test for cerebrovascular reactivity differences between the vehicle and Kaempferol treated TBI groups were determined by a two-way t-test corrected for multiple comparisons yielded no significant clusters. Arrows indicates the site of fluid percussion TBI. A two-way t-test corrected for multiple comparisons between Kaempferol- and vehicle-treated TBI groups was performed and voxels with t-values >2; corresponding to a corrected $P < 0.05$ was used as a significance threshold. The TBI+Kaempferol vs TBI+vehicle group comparisons revealed no voxel clusters of significant differences (figure panel not shown).

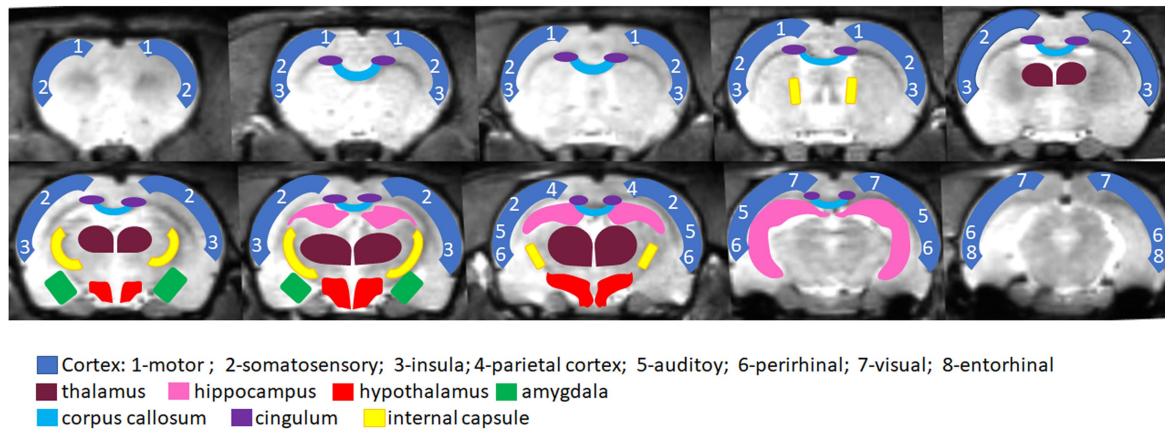
Supplementary Figure Caption:

Figure S1. Typical high-resolution sham T1 anatomical image linearly registered to the average sham rat brain template along with the various ROIs drawn after identification from the rat brain atlas.

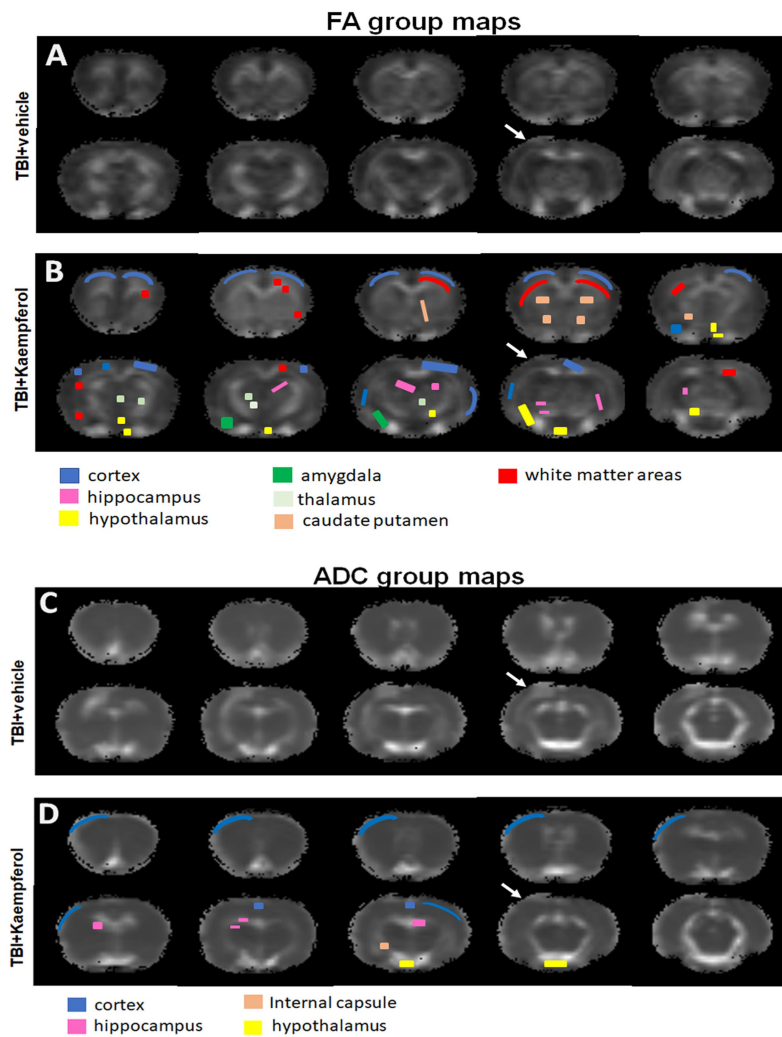


Figure S2. Group maps of DTI based FA and ADC during vehicle and Kaempferol treated conditions. **A.** FA vehicle group, **B.** FA Kaempferol treatment group, **C.** ADC vehicle group and **D.** ADC Kaempferol treated group. Areas exhibiting significant differences after Kaempferol treatment as obtained by statistical parametric mapping in **Figures 1A** and **1C** and described in results text are overlaid in color identifying the specific anatomical regions. Unilateral increases in FA were mostly within the ipsilateral perirhinal cortex, hippocampus, hypothalamus, thalamus and amygdala. However, bilateral FA increases were observed across motor, somatosensory cortices, insula and caudate putamen after Kaempferol treatment. Although ADC decrease (**panel D**) were relatively sparse compared to FA increase (**panel B**), highly specific ADC decreases occurred across ipsilateral cortical regions, hippocampus and bilaterally across the hypothalamus. Arrows indicate the location of fluid percussion TBI.